Dynamics and Similarity Laws for Adhering Vesicles in Haptotaxis

Isabelle Cantat and Chaouqi Misbah

Laboratoire de Spectrométrie Physique, Université Joseph Fourier (CNRS), Grenoble I, B.P. 87, Saint-Martin d'Hères, 38402 Cedex, France

(Received 18 September 1998)

We study vesicle dynamics induced by an adhesion gradient. This kind of migration is named haptotaxis in biology. The problem is fully solved as a free boundary one, including hydrodynamics flows. First, we analyze adhesion at equilibrium. We then determine the propulsion velocity as a function of various parameters. We find a persistent mixture of rolling and sliding. Similarity laws are extracted analytically both for the adhesion area and propulsion velocity by means of dimensional and scaling arguments. Our results markedly differ from classical results of nondeformable migrating entities.

PACS numbers: 87.16.–b, 47.55.Dz, 87.19.–j

Vesicles are closed membranes suspended in aqueous solution. Extensive investigations have been devoted to their equilibrium properties to date [1]. There are several circumstances in living systems where nonequilibrium features play a decisive role, however. Of particular interest is vesicle movement under external forces. A major leitmotiv in biological and medical science is the understanding of how and by which mechanisms cells of the immune system (e.g., granulocytes) move in response to tissue injury. This has led to the development of a number of experiments *in vitro* where cells are subject to external perturbations (e.g., shear flow). This step is essential in identifying the energetic, and possibly the kinetic, properties that are involved in displacing cells upon application of external forces when they are initially under adhesion on a substrate.

In this Letter, we present analytical and numerical results on vesicle dynamics in an adhesion gradient (haptotaxis). Our results can also be applied to situations where movement is due to the presence of a chemoattractant (chemotaxis).

Vesicle mobility induces a coupling of the flow within the membrane to the bulk fluid. With the help of Green's tensor techniques, we solve this free-boundary-like problem numerically and determine both the shape and velocity in haptotaxis. A close inspection of the underlying physical mechanisms allows us to extract analytically similarity laws for the adhesion area and vesicle velocity as functions of relevant parameters. These laws are in good agreement with the full numerical results. They should constitute an important basis for experimental studies. The numerical work is performed in two dimensions. The analytical scaling laws will be written, however, for both 2D and 3D.

The various sources of dissipations are the following. First, the internal dissipation due to phospholipidic molecules rotation characterized by the Leslie coefficient occurs on a very small time scale (typically 10^{-5} s), and is then negligible. In turn hydrodynamics relaxation occurs on the scale of 10^{-1} s (this time is obtained with the curvature rigidity, the water viscosity, and the vesicle size), and constitutes the first noticeable slow process for vesicle dynamics. Other sources of dissipations such as bond breaking and restoring associated with adhesion may become important and are currently under investigation.

Because the Reynolds number is typically small (Re $\sim 10^{-4}$), the Stokes approximation is justified. The hydrodynamics equations thus take the form

$$\eta \Delta \mathbf{v} = \nabla p; \qquad \nabla \cdot \mathbf{v} = 0. \tag{1}$$

We require continuity of $\mathbf{v}$ through the membrane and a vanishing velocity on the substratum; both demands express the no-slip condition and impermeability. The thin fluid film between the vesicle and the substratum is treated as in the bulk.

Thanks to linearity of the Stokes equations we can make use of the Green's function method. When viscosities inside and outside the vesicle are identical, the velocity field takes the form

$$\mathbf{v}(\mathbf{r},t) = \int_{\mathrm{memb}} \overline{\overline{T}} \cdot \mathbf{f}'_{\mathrm{memb}}\, ds' + \int_{\mathrm{subs}} \overline{\overline{T}} \cdot \left(-\eta \frac{\partial \mathbf{v}'}{\partial y'} + p' \hat{\mathbf{y}} \right) dx'. \tag{2}$$

Here $\overline{\overline{T}}$ is the Oseen tensor [2] and $\hat{\mathbf{y}}$ is a unit vector. For brevity we set $\mathbf{v}' \equiv \mathbf{v}(\mathbf{r}',t)$ and $\overline{\overline{T}} \equiv \overline{\overline{T}}(\mathbf{r},\mathbf{r}')$. The first term in Eq. (2) represents the membrane contribution, with $\mathbf{f}_{\mathrm{memb}}$ the membrane forces, to be specified below. The second term accounts for the presence of the adhesion wall parametrized by x'. It is worth mention that use could be made of the special Green's tensor taking into account the presence of the substratum [3]. In that case the second term in Eq. (2) disappears at the expense of a more complicated tensor.

The total force on the membrane is given by

$$\mathbf{f}_{\mathrm{memb}} = -\frac{\delta F}{\delta \mathbf{r}} = -\frac{\delta}{\delta \mathbf{r}} \int ds \left[\frac{\kappa}{2} c^2 + \zeta + w(\mathbf{r}(s)) \right] = \left[\left(\kappa \frac{\partial^2 c}{\partial s^2} + \frac{c^3}{2} \right) - c\zeta - \frac{\partial w}{\partial n}(\mathbf{r}) - cw(\mathbf{r}) \right] \mathbf{n} + \frac{\partial \zeta}{\partial s} \mathbf{t} . \tag{3}$$

Here $\mathbf{n}$ and $\mathbf{t}$ are the outward normal and the tangent to the vesicle; ζ is a time and space dependent Lagrange multiplier enforcing a constant local length [whereas area conservation in implied by Eq. (1)]; c denotes the membrane curvature, and κ the rigidity. Finally, $w(\mathbf{r})$ is the adhesion potential. For definiteness, if (x, y) are the coordinates along and perpendicular to the wall we take

$$w(\mathbf{r}) = [w_0 + (x - x_m)\nabla w]\{(d_0/y)^2[(d_0/y)^2 - 2]\} . \tag{4}$$

The potential is repulsive as $1/y^4$ for $y \ll d_0$ and attractive as $-1/y^2$ at long distance. The optimal distance $d_0 \sim 50$ nm between membrane and wall is constant. The prefactor depends linearly on x with a constant gradient ∇w. The mean value of the potential under the vesicle is also a constant w_0, and x_m is the middle point of the adhesion area and is thus moving in the laboratory frame. The vesicle is moving, thanks to an adhesion gradient. If the adhesion potential were fixed, the vesicle would experience an increasing adhesion during its movement. To avoid this we consider that $w(\mathbf{r})$ is invariant in the vesicle frame represented by x_m.

The numerical strategy is as follows. We first take the limit on the external variable $\mathbf{r}_{\mathbf{subs}}$ and set the left-hand side of Eq. (2) to zero. The force on substrate is obtained by inverting the integral equation. This determines $\mathbf{v}$ everywhere, and especially on the membrane. Dynamics are treated by forward iteration in time. These steps involve several technical points which will not be exposed here.

Thus, after transient have decayed, the vesicle acquires a permanent regime with a constant drift velocity, a situation on which we focus now. First, our numerical results predict velocities which lie in the range 0.1–10 μm/s for adhesion differences on both sides of the vesicle of about $\delta w/w_0 = 10\%$ [$R = 1$–10 μm (vesicle size), $\kappa = 20$–40 kT, $w = 10^2$–10^4 kT/μm]. It is a bit surprising that this value falls in the biological range. For example, granulocytes move at about 50 μm/s *in vivo* [4]. Another important feature is the persistent mixture between a rolling and a sliding motion (that is, the contact area has a small relative motion with respect to the substrate) (Fig. 1). The vesicle deformability and its adhesion length are crucial to capture this feature, because a rigid cylinder pulled parallel to a wall feels no torque, and thus only slides [5].

The type of motion (sliding and rolling) found here has been observed by Bongrand *et al.* for cells under shear flow [6]. Our results are in a marked contrast with theories imposing nonrealistic rigid bodies for cells [7]. The ability for the vesicle (or cell) to deform implies that the drift velocity obeys a nontrivial scaling law R^{-2} (in 3D) and $R^{-4/5}$ (in 2D) with the scale of the vesicle (see below and Fig. 4). The rigid body constraint leads to a quite different finding, namely the velocity scales as R^{-1} for a sphere (up to logarithmic corrections) [7], and as $R^{-1/2}$ for a cylinder [5].

Because of the complexity of the present problem it is highly desirable to have at our disposal analytical results. This is very important in order to get insight towards the understanding of the underlying physical ingredients which are responsible for vesicle dynamics. This is what we would like to sketch now.

A relevant parameter for the vesicle mobility on a substrate is the contact area. Let us first consider the 2D case as in the numerical work. The adhesion length (see Fig. 1 for definition) is well defined as long as $d_0 \ll R$ and is denoted by L_{adh}. Let us evaluate this quantity. L_{adh} depends only on the three characteristic lengths: $R = \frac{L}{2\pi}$, $R_s = \sqrt{A/\pi}$ corresponding to the vesicle perimeter L and area A, respectively, and $R_c = \sqrt{\kappa/w_0}$ which is related to the contact curvature [8]. We assume that L_{adh} has a weak dependence on velocity, an assumption which turns out to be quite legitimate in haptotaxis according to full numerical results. Typically three situations may occur, and we consider them separately.

(A) $R \gg R_c$: This situation is relevant in the case of a strong adhesion, and/or small rigidity, and/or giant vesicles. In reality, only the combination of these three facts matters. In that case the part of vesicle which is not in contact with the substrate is a truncated quasicircular shape with angular contact point. Indeed if the rigidity is negligible in comparison to the adhesion, we recover the fluidlike droplet model [1]. L_{adh} can thus be expressed analytically in the limit $R_s/R \to 1$ (a situation often encountered in real situations) as

$$L_{\mathrm{adh}} \sim R(1 - R_s/R)^{1/3} . \tag{5}$$

We have explored numerically this regime. Figure 2 shows the analytical part compared to the numerical one. The agreement is quite satisfactory. The other limit $R_s/R \to 0$ (small swelling) yields obviously $L_{\mathrm{adh}} = L/2$.

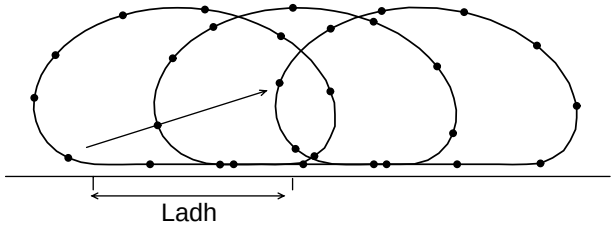

FIG. 1. Vesicle shape at three different times. The arrow indicates the trajectory of a material point on the vesicle illustrating the rolling and sliding motion.

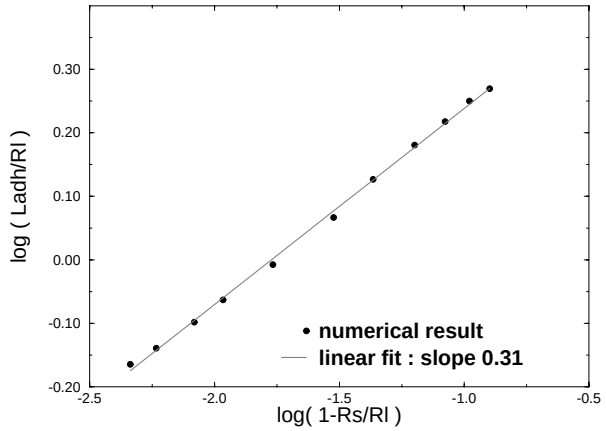

FIG. 2. Variation of adhesion length with the swelling. (Numerical parameters: $R = 1.1$ and $R_c = 0.6$, with an arbitrary unit of length.)

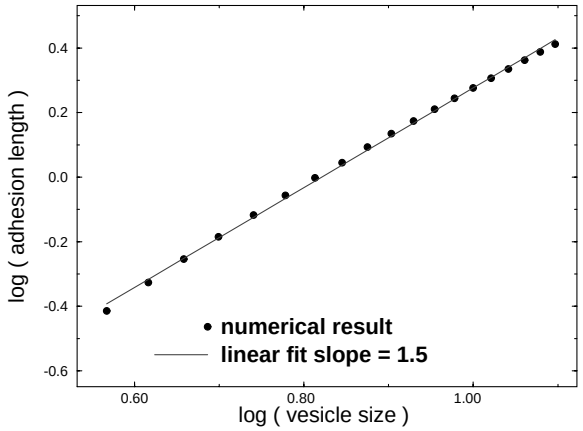

FIG. 3. Variation of adhesion length with the vesicle size. [Numerical parameters: $R_s/R = 0.9$ and $R_c = 1.2$ (arbitrary unit)].

(B) $R_c \sim R$: This situation corresponds to the case of intermediate rigidity, or more precisely when all effects compete. This case is more subtle. At equilibrium, the increase in curvature energy due to adhesion must be offset by the decrease in the adhesion energy. The evaluation of both terms will provide us with a scaling law for L_{adh}. For that purpose, let $\delta c(s)$ denote the curvature variation between the free and adhering vesicle, which is supposed swelled ($R_s \sim R$) and impermeable. The conservation of vesicle perimeter under such a variation entails a vanishing mean value for $\delta c(s)$. Therefore the global curvature energy variation is proportional to $\int \kappa(\delta c)^2\, ds$. We evaluate δc by means of the volume conservation condition. Under adhesion the volume deficit (the area in 2D) which is beneath, $\delta v \sim L_{\mathrm{adh}}^3/R$, must be redistributed elsewhere, so as to keep the total volume constant. The estimate for δv is performed on a portion of a disc with a radius R and a base L_{adh} in the limit of small enough L_{adh} as compared to the total length; see Fig. 4. That is, we consider the equivalent disc of the real shape. Because a disc has a larger volume, it must be truncated by a quantity δv. This amounts to the sought after curvature increase, since the truncated object has a smaller effective radius of curvature. This leads to a radius increase $\delta R \sim \delta v/R \sim R^2 \delta c$. This implies that the increase in curvature energy is $\Delta E_c \sim \kappa L_{\mathrm{adh}}^6/R^7$. The variation of the adhesion energy is simply given by $\Delta E_w \sim w_0 L_{\mathrm{adh}}$. A balance between ΔE_c and ΔE_w yields

$$L_{\mathrm{adh}} \sim \left(\frac{w_0}{\kappa}\right)^{1/5} R^{7/5}. \tag{6}$$

The same arguments can be extended to 3D providing us with

$$L_{\mathrm{adh}} \sim \left(\frac{w_0}{\kappa}\right)^{1/6} R^{4/3}. \tag{7}$$

The full numerical analysis provides a good agreement with the scaling laws (Fig. 3). Higher values of R will cause a crossover to the behavior in Fig. 2, while smaller values lead to vesicle unbinding (see below), so that the validity of the scaling law is limited by these two physical facts.

(C) $R_c > R$: This is the weak adhesion limit close to the unbinding transition already analyzed in [8]. Since we do not address here the problem of unbinding this limit will not be considered later.

Having determined the adhesion length, we are in a position to study dynamics. In this brief exposition we shall limit ourselves to the situation of intermediate adhesion. Energy is injected by adhesion gradients, and is dissipated in hydrodynamics flows. Let us first evaluate the viscous dissipation.

The largest velocity gradients occur in the fluid influenced by both the vesicle and the substrate. Note that the dissipation in the thin fluid film between the vesicle and the substrate is limited by the great rolling ratio. For simplicity we assume that the vesicle is in direct contact with the substrate (no fluid film beneath). The volume of dissipation is that corresponding to the influence region, and scales as L_{adh}^2 (as is the case with Laplacian fields—we have $\nabla^2 p = 0$—the perturbation penetrates over a scale of order L_{adh} in the two directions). In these regions (see Fig. 4) the mean local velocity is estimated at a distance L_{adh} from the contact point (in the fluid bulk) as $V_{\mathrm{loc}} \sim V L_{\mathrm{adh}}/R$ using a rolling without sliding motion. This relation is geometrically obvious from Fig. 4 for a small adhesion length. If

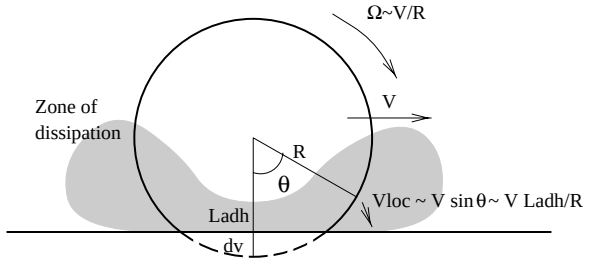

FIG. 4. Definition and schematic views of several quantities used in the analytical part.

this is not the case, it is clear on the general ground that since the vesicle must adhere on a length $L_{\rm adh}$ the typical velocity gradient must be set on that range, and is equal to $V_{\rm loc}/L_{\rm adh}$. On the global scale of the vesicle the gradient is V/R. The demand that a permanent regime is established requires the two gradients to scale in the same manner, namely $V_{\rm loc}/L_{\rm adh} \sim V/R$ (these correspond to the inverse of time scales for dissipation), which is a more profound physical view of the relation introduced above. Note also that the greater the adhesion length, the larger is $V_{\rm loc}$ for a given R and V. This is obvious since the vesicle must evacuate the fluid on a larger length, and in order to move at the same global velocity V, $V_{\rm loc}$ must be larger.

Using the dependence $R^{7/5}$ for $L_{\rm adh}$ [Eq. (6)] we deduce the functional dependence of the dissipation (in 2D):

$$D \sim \eta L_{\rm adh}^2 \left(\frac{V_{\rm loc}}{L_{\rm adh}}\right)^2 \sim \eta V^2 \left(\frac{R}{R_c}\right)^{4/5}. \qquad (8)$$

Equating dissipation, D, and source, $F_d V$, with F_d the driving force, we arrive at

$$V \sim \frac{F_d}{\eta}\left(\frac{R_c}{R}\right)^{4/5} \quad (2{\rm D}), \qquad V \sim \frac{F_d}{\eta}\frac{R_c}{R^2} \quad (3{\rm D}). \qquad (9)$$

For 3D, dissipation occurs in a volume $L_{\rm adh}^3$, and $L_{\rm adh}$ obeys different scaling [Eq. (7)]. This implies a different dependence on R.

This law works for any driving force F_d. In 2D the force is defined per unit length. In haptotaxis $\mathbf{F}_d = L_{\rm adh}\nabla w$ in 2D and $\mathbf{F}_d = L_{\rm adh}^2 \nabla w$ in 3D. Comparison with full numerics is presented on Fig. 5. The best fit provides (over about a decade) 0.75 ± 0.05, while full analytical results predict $4/5 = 0.8$. It is very important to note that theories with rigid bodies [7] lead to $V \sim R^{-1}$ in 3D and $V \sim R^{-1/2}$ in 2D. Allowing for vesicle deformability leads to the nontrivial law R^{-2} and $R^{-4/5}$ in 3D and 2D, respectively.

Further increase of R leads (as for statics discussed before) to a crossover to a strongly adhering regime discussed below. In the extreme limit of tensely adhering vesicles, and if the swelling is large, $L_{\rm adh}$ is given by Eq. (5). We can derive the drift velocity in the same manner. Because $L_{\rm adh}$ is proportional to the vesicle scale R, and given the form of dissipation and source powers discussed above, we obtain for the drift velocity

$$V \sim F_d/\eta \quad (2{\rm D}), \qquad V \sim F_d/(\eta R) \quad (3{\rm D}). \qquad (10)$$

We obtain here for 2D and 3D similar results as for a cylinder and a sphere (Stokes law) immersed in an infinite medium (no substrate). We hope to report on extensive numerical results in the future.

The next step will be to extend the numerical treatment to 3D. In addition, the relevance of several physical points should be clarified in the future. (i) We have taken into account the first natural dissipation associated with hydrodynamical flow inside and outside the vesicle. This assumes that the two monolayers form an entity, in that they do not slide with respect to each other. It is likely [9] that this is not always true, and the effect of the induced dissipation should be investigated in the future. (ii) Furthermore, perhaps the most serious point that must be emphasized with regard to dissipation in the realm of biology concerns the kinetics of bond breaking and restoring with the substrate. If the time scale involved in this process is larger than that associated with hydrodynamics, dissipation should be dominated by chemical kinetics. The time scale depends on the energetics involved in the adhesion, and it seems at first sight that in the biological world the bond breaking dynamics should be of great importance [10]. (iii) Finally, in order to be closer to realistic situations we should relax the assumption of equal viscosities inside and outside the vesicle. In reality, the cytoskeleton exhibits viscoelastic properties that are necessary to incorporate in future models which are aiming at a more elaborate theory of cell motility.

We are very grateful to R. Bruinsma, F. Jülicher, and U. Seifert for several enlightening and stimulating discussions.

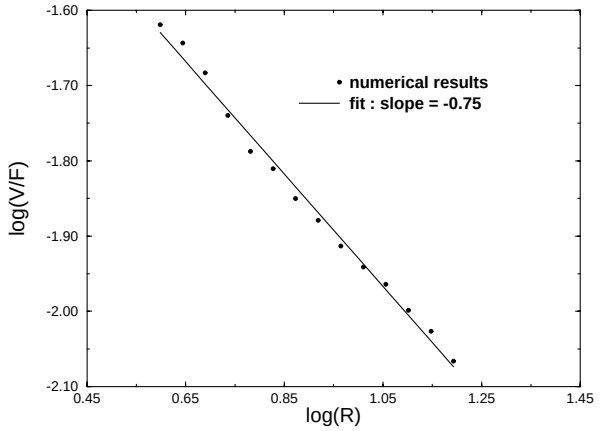

FIG. 5. Variation of the ratio (velocity/driving force) with the scale at constant swelling. [$R_s/R = 0.95$, $R_c = 0.5$, $\nabla w/w_0 = 0.2$, and $d_0 = 0.06$ (arbitrary units)].

[1] *Structure and Dynamics of Membranes, Handbook of Biological Physics,* edited by R. Lipowsky and E. Sackmann (Elsevier, Amsterdam, 1995).
[2] O. A. Ladyzhenskaya, *The Mathematical Theory of Viscous Incompresible Flow* (Gordon and Breach, New York, 1969), 2nd ed., Chap. 3.
[3] J. R. Blake, Proc. Cambridge Philos. Soc. **70**, 303 (1971).
[4] M. B. Lawrence and T. A. Springer, Cell **65**, 859 (1991).
[5] D. J. Jeffrey and Y. Onishi, Q. J. Mech. Appl. Math. **34**, 129 (1981).
[6] O. Tissot, A. Pierres, C. Foa, M. Delaage, and P. Bongrand, Biophys. J. **61**, 204 (1992).
[7] A. J. Goldman, R. G. Cox, and H. Brenner, Chem. Eng. Sci. **22**, 637 (1967).
[8] U. Seifert, Phys. Rev. A **43**, 6803 (1991).
[9] U. Seifert and S. A. Langer, Europhys. Lett. **23**, 71 (1993).
[10] R. Bruinsma, in *Physics of Biomaterials, Fluctuations, Self Assembly and Evolution,* edited by T. Risk and D. Sherrington, NATO ASI Ser. 332 (Kluwer, Dordrecht, 1996).